M $^{\text{odeling}}$ MC $^{\text{omputing}}$ $_{\text{athematical}}$

Oblique stagnation-point flow of ternary hybrid nanofluid towards a shrinking surface

Rozaidi N. L.[1], Hafidzuddin M. E. H.[1,2], Arifin N. M.[1], Ab Ghani A.[1]

[1]*Department of Mathematics and Statistics, Universiti Putra Malaysia,*
43400 Serdang, Selangor, Malaysia
[2]*Centre For Foundation Studies in Science Of Universiti Putra Malaysia,*
43400 Serdang, Selangor, Malaysia

The oblique stagnation-point flow of a ternary hybrid nanofluid towards a shrinking surface is studied numerically in this paper. A similarity transformation was used to convert the governing equations into a set of ordinary differential equations, which were then solved numerically using the bvp4c solver in MATLAB software. The research, involving three different nanoparticles, provides valuable insights into their impact on the fluid dynamics and heat transfer characteristics of the system under study. The influence of the parameters S, λ and nanoparticle volume fraction on velocity and temperature profiles, local skin friction and local Nusselt number are discussed and presented in tabular and graphical forms. It is found that higher nanoparticle concentrations lead to increased resistance to flow, convection, and heat transfer rates.

Keywords: *natural convection flow; Al_2O_3-Cu/water hybrid nanofluid; square cavity; finite element method; nanoparticle shape.*

1. Introduction

In fluid dynamics, stagnation-point flow refers to the flow near a stagnation streamline that occurs when a fluid impinges on a surface orthogonally. The stagnation point marks the location where the oncoming flow divides to pass on either side of the surface. Hiemenz [1] was the first to find that the Navier–Stokes equations can precisely analyse stagnation-point flow via similarity transformation. The conventional two-dimensional stagnation-point flow also has been explored, which describes the flow of fluid orthogonally striking a solid surface. The solid surface can be stationary or have a stretching or shrinking velocity. This type of flow is encountered in various applications such as the cooling process of nuclear reactors and electronic devices, polymer and plastic extrusion, and wire drawing. In some situations, the flow impinges obliquely on the solid surface, resulting in oblique stagnation-point flow, which refers to the flow of a fluid towards a solid surface where the flow impinges obliquely (at an angle) instead of directly normal to the surface. It is a specific case of stagnation-point flow, which occurs when the flow velocity of the fluid becomes zero at a certain point on the surface. The oblique stagnation-point flow and radiative heat transfer of an incompressible viscous fluid towards a shrinking sheet was studied by Mahapatra et al. [2], to which they found that the temperature at a point in the fluid decreases with increase in effective Prandtl number.

Nanofluids, which are created by incorporating nano-sized particles into conventional fluids such as water, ethylene glycol, and oils, have gained significant attention due to their enhanced thermal conductivity properties. Researchers have examined the effects of different parameters, such as nanoparticle concentration, nanoparticle size, fluid viscosity, and surface conditions, on the heat transfer performance and flow properties in oblique stagnation point flow of nanofluids. The exploration of nanofluids has been the subject of extensive research efforts, aiming to understand and leverage their unique properties for practical applications. In the research of the laminar two-dimensional stagnation-point flow and heat transfer of a viscous incompressible nanofluid obliquely impinging on a shrinking surface

done by Rahman et al. [3], it is found that dimensionless strain rate and shrinking parameter cause a shift in the position of the point of zero skin friction along the stretching sheet. They also discovered that the obliquity of the flow toward the surface increases as the strain rate intensifies. Furthermore, Khan [4] analysed the heat transfer characteristics and the flow properties for two-dimensional oblique stagnation point flow of viscous, incompressible nanofluid over a curved stretching/shrinking surface. In his analysis, he confirmed that the addition of nanoparticles to base fluid strengthens the drag force and lowers the heat transfer rate at the surface.

A hybrid nanofluid refers to a type of nanofluid that is created by combining two or more different types of nanoparticles in a base fluid, typically one metallic and one non-metallic, with conventional heat transfer fluids. The non-metallic nanoparticles offer advantages such as chemical inertness and stability, although they have lower thermal conductivity. This combination allows for a more efficient transfer of heat in various applications. Suresh et al. [5] conducted an experimental work where they investigated a fully developed laminar convective heat transfer and pressure drop characteristics through a uniformly heated circular tube using Al_2O_3-Cu/water hybrid nanofluid. Their work resulted in 0.1% Al_2O_3-Cu/water hybrid nanofluids have slightly higher friction factor when compared to 0.1% Al_2O_3/water nanofluid. Sidik et al. [6] stated that hybrid nanofluids have shown enhanced thermal characteristics compared to base fluids and single-nanoparticle fluids. Stability is crucial for hybrid nanofluids, and surfactants play a role in dispersibility but can affect viscosity and thermal conductivity. Insufficient stability can have adverse effects on the nanofluid.

In another study, Abuzar et al. [7] investigated the combined effect of radiation and convective boundary conditions in the region of oblique stagnation point flow. They discovered that the increasing values of Biot number imply the enhancement in heat transfer, thermal boundary layer thickness, and concentration boundary layer thickness. In 2017, a new modeled thermophysical properties have been proposed by Devi dan Devi [8] to investigate the effects of a magnetic field on the flow of a water-based Al_2O_3-Cu hybrid nanofluid over a permeable sheet with a stretching velocity. The new properties were found to be in good agreement with the experimental results obtained in [5]. Later, Hayat et al. [9] examined and compared the improvement of flow and heat transfer characteristics between a rotating nanofluid and a newly discovered hybrid nanofluid in the presence of velocity slip and thermal slip. It was discovered that the heat transfer rate of the hybrid nanofluid is higher as compared to the traditional nanofluid. Next, a numerical solution for laminar, incompressible, and steady oblique stagnation point flow of Cu-water nanofluid over a stretching/shrinking sheet with mass suction S was considered by Li et al. [10]. They found that the streamline pattern is not symmetric, and reversed phenomenon is detected close to the shrinking surface. Furthermore, they also observed that the free stream parameter changes the direction of the oncoming flow and controls the obliqueness of the flow.

A ternary hybrid nanofluid refers to a type of nanofluid that is composed of three different types of nanoparticles dispersed in a base fluid. These nanoparticles can be of various compositions, such as different metals, metal oxides, carbon-based materials or a combination of them. Researchers study ternary hybrid nanofluids to optimize characteristics such as thermal conductivity and heat transfer performance. These nanofluids have applications in areas such as thermal management systems and electronic cooling. In an exploration of ternary-hybrid nanofluid experiencing Coriolis and Lorentz forces: case of three-dimensional flow of water conveying carbon nanotubes, graphene, and alumina nanoparticles conducted by Oke et al. [11], they concluded that the stretching parameter decelerates the flow of the ternary hybrid nanofluid in the x direction and lowers the surface temperature, whereas there is enhancement of the velocity field in the y direction with growth in the stretching parameter.

In the following year, Mahmood and Khan [12] carried out a study on the numerical analysis of an unstable three-dimensional (3D) nodal stagnation point flow of a polymer-based ternary nanofluid (Al_2O_3-CuO-TiO_2/polymer) over a stretching surface, considering the effects of mass suction and heat source, to which they concluded that the heat transfer presentation of ternary-hybrid nanofluid has superior to the hybrid nanofluid and the normal nanofluid for the suction parameter. In the paper published by Sajid et al. [13], their focus was on the motion of ternary hybrid nanofluids inside a porous

rotating disk. The novelity in their study is that the extension in Yamada–Ota and Xue nanofluid models in the case of tri-hybrid nanoparticles has never studied before in the existing literature. They learned that the insertion of trihybrid nanoparticles instead of dihybrid nanomolecules in the standard liquid boosts the thermal conduction effect and temperature inside the fluid which ultimately escalates the heat deliverance rate. Meanwhile, the potential practical applications of a ternary hybrid nanofluid in the presence of suction and Lorentz force was studied by [14]. The flow through a stagnation zone of a stretching or shrinking curved surface were considered. The results showed that in the presence of a magnetic field and suction, the velocity was enhanced, while it was reduced by curvature and nanoparticle volume fraction for both stretching and shrinking surfaces. The study revealed that changing the suction parameters from 2.0 to 2.5 leads to an increase in heat transfer rates ranging from 34% to 35%. This proves that the presence of ternary hybrid nanofluids contributes to improved velocity and temperature distributions. Recently, Yahaya et al. [15] analysed the effects of suction on the oblique stagnation-point flow of hybrid nanofluid Cu-Al$_2$O$_3$/H$_2$O over a shrinking surface, and they learned that the rise in the suction parameter augments the normal and shear components of skin friction and enhances the velocity profiles for both normal and shear flows.

In this study, we extend the work done in [15] by considering the numerical solution of the oblique stagnation-point of ternary hybrid nanofluid towards a shrinking surface. The methodology, results, discussion, as well as the conclusion of our work are detailed in the following section.

2. Problem formulation

A steady two-dimensional hybrid nanofluid flow that impinges obliquely on a surface is considered, as illustrated in Figure 1. The Cartesian coordinates (x, y) are used to denote the regions parallel and normal to the surface. The x-axis is aligned parallel to the shrinking surface, while the y-axis is perpendicular to it. The flow occurs in the region where $y \geqslant 0$. The surface velocity is described by the function $u_s(x) = ax$, where a represents the coefficient of the velocity profile. A value of $a = 0$ corresponds to a static surface, while $a < 0$ indicates a shrinking surface. The mass flux velocity on the shrinking surface is denoted as v_s, with negative values

Fig. 1. Illustration of stagnation-point flow field.

indicating suction and positive values indicating injection. The external flow is assumed to be a combination of a simple shear flow and an ortho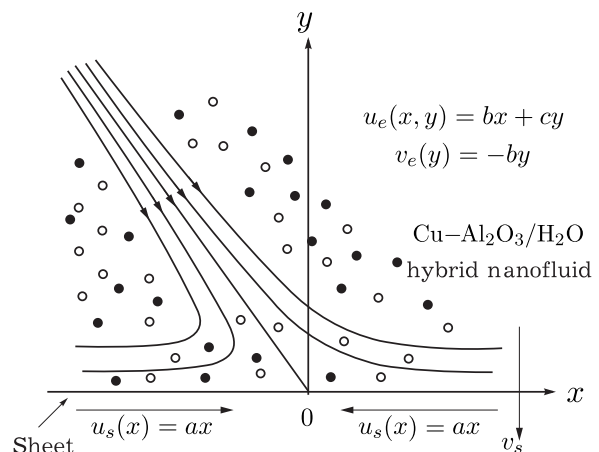gonal stagnation-point flow. The flow is represented by a stream function, denoted as ψ, and it is defined by the constants a and b,

$$\psi = bxy + \frac{1}{2}cy^2$$

The external velocities are given by $u_e(x, y) = bx + cy$ and $v_e(y) = -by$. The surface temperature of the flow is assumed to be constant and denoted as T_s, while T_∞ represents the temperature of the surrounding ambient hybrid nanofluid.

With the above-mentioned assumptions, the governing boundary layer equations in the forms of partial differential equation, which are based on he basic physical concepts including momentum, energy and continuity equations are listed as follows [15]

$$\frac{\partial u}{\partial x} + \frac{\partial v}{\partial y} = 0, \tag{1}$$

$$u\frac{\partial u}{\partial x} + v\frac{\partial u}{\partial y} = -\frac{1}{\rho_{mnf}}\frac{\partial p}{\partial x} + \frac{\mu_{mnf}}{\rho_{mnf}}\left(\frac{\partial^2 u}{\partial x^2} + \frac{\partial^2 u}{\partial y^2}\right), \tag{2}$$

$$u\frac{\partial v}{\partial x} + v\frac{\partial v}{\partial y} = -\frac{1}{\rho_{mnf}}\frac{\partial p}{\partial x} + \frac{\mu_{mnf}}{\rho_{mnf}}\left(\frac{\partial^2 v}{\partial x^2} + \frac{\partial^2 v}{\partial y^2}\right), \tag{3}$$

$$u\frac{\partial T}{\partial x} + v\frac{\partial T}{\partial y} = \frac{k_{mnf}}{(\rho C_p)_{mnf}}\frac{\partial p}{\partial x} + \left(\frac{\partial^2 T}{\partial x^2} + \frac{\partial^2 T}{\partial y^2}\right), \tag{4}$$

along with following boundary conditions

$$\begin{aligned}
\frac{\partial \psi}{\partial x} &= -v_s, \quad \frac{\partial \psi}{\partial y} = u_s, \quad T = T_w \quad \text{at} \quad y = 0, \\
\frac{\partial \psi}{\partial x} &= -v_e, \quad \frac{\partial \psi}{\partial y} = u_e, \quad T \to T_\infty \quad \text{at} \quad y \to \infty,
\end{aligned} \tag{5}$$

where μ_{mnf} is the dynamic viscosity, ρ_{mnf} is the density of ternary hybrid nanofluid, p is the pressure, T is the temperature of ternary hybrid nanofluid, k_{mnf} is the thermal conductivity of ternary hybrid nanofluid and $(\rho C_p)_{mnf}$ is the heat capacity of the ternary hybrid nanofluid.

Table 1. Ternary hybrid nanofluid's thermal properties.

Properties	Ternary hybrid nanofluid
Density	$\rho_{mnf} = (1-\phi_3)\{(1-\phi_2)[(1-\phi_1)\rho_f + \phi_1\rho_{s1}] + \phi_2\rho_{s2}\} + \phi_3\rho_{s3}$
Dynamic Viscocity	$\mu_{mnf} = \dfrac{\mu_f}{(1-\phi_3)^{2.5}(1-\phi_2)^{2.5}(1-\phi_1)^{2.5}}$
Thermal Conductivity	$\dfrac{k_{mnf}}{k_{hnf}} = \dfrac{k_{s3} + (m-1)k_{hnf} - (m-1)\phi_3(k_{hnf} - k_{s3})}{k_{s3} + (m-1)k_{hnf} + \phi_3(k_{hnf} - k_{s3})}$
	$\dfrac{k_{hnf}}{k_{nf}} = \dfrac{k_{s2} + (m-1)k_{nf} - (m-1)\phi_2(k_{nf} - k_{s2})}{k_{s2} + (m-1)k_{nf} + \phi_2(k_{nf} - k_{s2})}$
	$\dfrac{k_{nf}}{k_f} = \dfrac{k_{s1} + (m-1)k_f - (m-1)\phi_1(k_f - k_{s1})}{k_{s1} + (m-1)k_f + \phi_1(k_f - k_{s1})}$
Heat Capacity	$(\rho C_p)_{mnf} = (1-\phi_3)\{(1-\phi_2)[(1-\phi_1)(\rho C_p)_f + \phi_1(\rho C_p)_{s1}] + \phi_2(\rho C_p)_{s2}\} + \phi_3(\rho C_p)_{s3}$
Electrical Conductivity	$\dfrac{\sigma_{mnf}}{\sigma_{hnf}} = \dfrac{k_{s3} + 2\sigma_{hnf} - 2\phi_3(\sigma_{hnf} - \sigma_{s3})}{\sigma_{s3} + 2\sigma_{hnf} + \phi_3(\sigma_{hnf} - \sigma_{s3})}$
	$\dfrac{\sigma_{hnf}}{\sigma_{nf}} = \dfrac{\sigma_{s2} + 2\sigma_{nf} - 2\phi_2(\sigma_{nf} - \sigma_{s2})}{\sigma_{s2} + 2\sigma_{nf} + \phi_2(\sigma_{nf} - \sigma_{s2})}$
	$\dfrac{\sigma_{nf}}{\sigma_f} = \dfrac{\sigma_{s1} + 2\sigma_f - 2\phi_1(\sigma_f - \sigma_{s1})}{\sigma_{s1} + 2\sigma_f + \phi_1(\sigma_f - \sigma_{s1})}$

Table 1 lists the thermal properties of ternary hybrid nanofluid where ϕ_1, ϕ_2 and ϕ_3 represent the solid volume fractions of nanoparticles, namely as Cu, Fe_3O_4 and SiO_2. The four types of fluids which are ternary hybrid nanofluids, hybrid nanofluids, nanofluids, and fluids are also indicated by the subscripts mnf, hnf, nf and f, respectively. Besides, subscripts $s1$, $s2$ and $s3$ stands for denoting the properties of Cu, Fe_3O_4 and SiO_2. Meanwhile, Table 2 lists the characteristics of copper, iron oxide, silicon dioxide and polymer as the base fluid along with various other thermophysical characteristics [16].

Table 2. Numerical values of polymer base and ternary hybrid nanoparticles.

Properties	Cu (ϕ_1)	Fe_3O_4 (ϕ_2)	SiO_2 (ϕ_3)	Polymer
ρ (kg/m^3)	8933	5180	2650	1060
C_p (J/kg K)	385	670	730	3770
k (W/m K)	401	9.7	1.5	0.429
σ (Ωm)$^{-1}$	$5.96 \cdot 10^7$	$2.5 \cdot 10^{-4}$	$1.0 \cdot 10^{-18}$	$4.3 \cdot 10^{-5}$
Pr				6.2

The similarity transformation is used to reduce the system of partial differential equations to ordinary differential equations. These transformations help reduce the number of independent variables

in the equations by at least one compared to the original system. The specific transformations used in the study are introduced as follows:

$$\psi = (b\nu_f)^{\frac{1}{2}} x f(\eta) + \frac{c\nu_f}{b} \int_0^\eta g(s)\, ds, \quad u = \frac{\partial \psi}{\partial y}, \quad v = -\frac{\partial \psi}{\partial x},$$

$$\eta = y\left(\frac{b}{\nu_f}\right)^{\frac{1}{2}}, \quad \theta(\eta) = \frac{T - T_\infty}{T_w - T_\infty}. \tag{6}$$

Employing the variables in the form (6), Eq. (1) is satisfied, while Eq. (2)–(4) are transformed to the following ordinary differential equations

$$\frac{\mu_{mnf}/\mu_f}{\rho_{mnf}/\rho_f} f^{iv} + f f''' - f' f'' = 0, \tag{7}$$

$$\frac{\mu_{mnf}/\mu_f}{\rho_{mnf}/\rho_f} g''' + f g'' - f'' g = 0, \tag{8}$$

$$\frac{1}{\mathrm{Pr}} \frac{k_{mnf}/k_f}{(\rho C_p)_{mnf}/(\rho C_p)_f} \theta'' + f \theta' = 0, \tag{9}$$

which associates with the following boundary conditions

$$f(0) = S, \quad f'(0) = \lambda, \quad g(0) = 0, \quad \theta(0) = 1,$$
$$f(\eta) \to 1, \quad g'(0) \to 1, \quad \theta(\eta) \to 0 \quad \text{as} \quad \eta \to \infty, \tag{10}$$

where S and λ denote suction ($S > 0$) or injection ($S < 0$) and shrinking ($\lambda < 0$) or stretching ($\lambda > 0$) surface, respectively.

The physical quantities of interest are local skin friction C_{fx} and Nusselt number, Nu_x which are given by

$$C_{fx} = \frac{\mu_{mnf}}{\rho_f (bx)^2} \left(\frac{\partial u}{\partial y}\right)_{y=0}, \quad Nu_x = -\frac{x k_{mnf}}{k_f (T_w - T_\infty)} \left(\frac{\partial T}{\partial y}\right)_{y=0}. \tag{11}$$

Using (6), Eqs. (11) become

$$\mathrm{Re}_x C_{fx} = \frac{\mu_{mnf}}{\mu_f} \left(\xi f''(0) + \frac{c}{b} g'(0)\right), \quad \mathrm{Re}_x^{-\frac{1}{2}} Nu_x = -\frac{k_{mnf}}{k_f} \theta'(0). \tag{12}$$

where $\mathrm{Re}_x = \frac{bx^2}{\nu_f} = \xi^2$ is the local Reynolds number.

3. Results and discussion

The bvp4c solver in the MATLAB software is used to numerically solve the individual equations, such as the momentum equation (7) and energy equation (9) along with the boundary conditions (10). Table 3 shows the relative values of $f''(0)$, with the various values of S and λ, $\phi_{\mathrm{Al_2O_3}}$ and ϕ_{Cu}, indicating a fair connection between the current results and the earlier studies [3] and [15]. As a result, the current numerical method can be employed confidently to address the current problem's fluid flow and heat transfer.

The values of $f''(0)$ in Table 3 are determined by solving Eqs. (7) and (9) subject to the boundary conditions (10). Suction parameter S values are varied within the range $0 \leqslant S \leqslant 2$ in order to examine how the fluid's flow and thermal behaviours are affected by the presence and increase of S. Meanwhile, the other controlling parameters are held constant at $m = 4.9$, $\phi_2 = \phi_3 = 0$ and $\mathrm{Pr} = 6.2$. This study refers to the thermophysical properties of hybrid carbon nanotubes obtained from the previous study [16] as shown in Table 1.

Figure 2 shows the effect of the suction parameter S on reduced skin friction, $f''(0)$. The figure portrays the result for three different types of nanoparticles with the various values of S. From the graph, it can be seen that the critical values, λ_c for $S = 0, 1, 2$ are $\lambda_c = -1.24658, -1.955797$ and -3.1155, respectively. It is noticed that the values of skin friction coefficient, $f''(0)$ increase as S increases. Meanwhile, Figure 3 illustrates the result of reduced skin friction $f''(0)$ with $\phi_1 = \phi_2 = \phi_3 = 0.01$ for different values of λ ($= -1.1, -1.2, -1.3$). It is noticed in both figures that dual solutions

Table 3. Values of $f''(0)$ with different values of S, λ, $\phi_{Al_2O_3}$, ϕ_{Cu} and $\mathrm{Pr} = 6.2$.

S	λ	$\phi_{Al_2O_3}$	ϕ_{Cu}	Ref. [3]		Ref. [15]		Present result	
				First	Second	First	Second	First	Second
0	0	0	0	0.6479004	—	0.647900	—	0.647900	—
	−0.8			1.5512911	—	1.551291	—	1.551291	—
	−1			1.9661288	—	1.966129	—	1.966129	—
	−1.1	0.05	0.05	—	—	2.085357	7.019518	2.085358	7.019521
1				—	—	0.061713	6.456471	0.061715	6.456472
2				—	—	−1.297665	4.204348	−1.297664	4.204350

are generated from different initial guesses made in the bvp4c solver. The solutions are referred to as the first and second solutions in the following results. The determination is made based on the convergence of these solutions to asymptotic behaviour when the free stream boundary conditions (10) are satisfied. The dual solutions are obtained for $S > S_c$ and $\lambda > \lambda_c$, while no solution for $S < S_c$ and $\lambda < \lambda_c$. Here, S_c and λ_c are the critical points at which a unique solution exists.
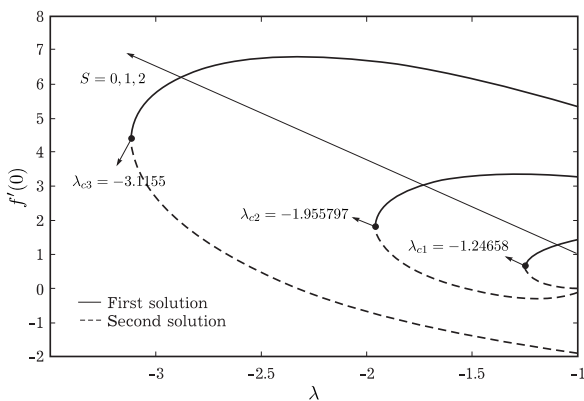

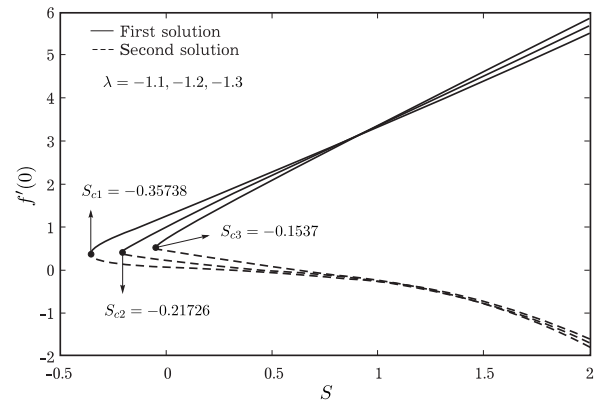**Fig. 2.** Effect of various S on reduced skin friction.

Fig. 3. Effect of various λ on reduced skin friction.
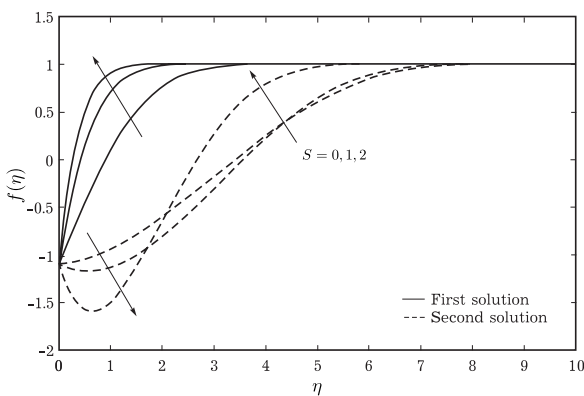

Fig. 4. Effect of various S on velocity profile $f'(\eta)$.
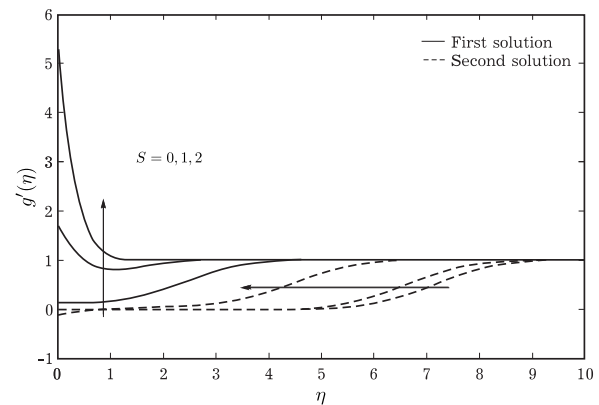

Fig. 5. Effect of various S on velocity profile $g'(\eta)$.

Figures 4–6 portray the variation of velocity profile, $f'(\eta)$ and $g'(\eta)$, and temperature profile, $\theta(\eta)$ for suction parameter which is S. These graphs focus on the results of several different nanoparticles which are $\phi_1 = \phi_2 = \phi_3 = 0.01$ for different values of $S (= 0, 1, 2)$. The value of parameter of λ is fixed to -1.1. Figures 4 and 5 show that the values of $f'(\eta)$ and $g'(\eta)$ increase with the increase of S and η. On the other hand, the values of $\theta(\eta)$ decrease with the increase of S and η, as depicted in Figure 6. As a result, the application of suction forces the ternary hybrid nanofluid to move closer to the surface, leading to a reduction in both momentum and thermal boundary layer thickness. The decrease in the momentum boundary layer thickness contributes to a delay in boundary layer separation. Additionally, it is observed that both the normal $f'(\eta)$ and shear $g'(\eta)$ flow velocities experience an increase with the imposition of suction.

Table 4 shows the various values of skin friction, C_f and Nusselt number, Nu_x with different values of ϕ_1, ϕ_2 and ϕ_3 with λ and S. Increasing the values of three different nanoparticles leads to an increase in both the Nusselt number and skin friction. The relationship between nanoparticle concentration and skin friction is more complex. The presence of nanoparticles in a fluid can alter its rheological properties, affecting viscosity. An increase in nanoparticle concentration may lead to changes in fluid viscosity, impacting the skin friction. Higher concentrations could potentially increase the resistance to flow, resulting in higher skin friction.

Fig. 6. Effect of various S on temperature profile $\theta(\eta)$.

Meanwhile, an increase in the nanoparticles concentration can enhance heat transfer due to improved thermal conductivity and increased surface area for heat exchange. Higher nanoparticle concentrations may lead to increased convection and heat transfer rates, resulting in a higher Nusselt number.
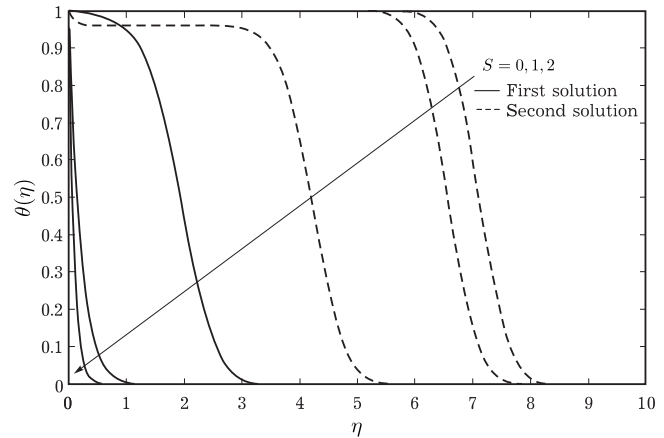
Table 4. Values of C_f and Nu_x with different values of ϕ_1, ϕ_2 and ϕ_3.

Cu	**Fe$_3$O$_4$**	**SiO$_2$**	Skin friction, C_f		Nusselt, Nu_x	
(ϕ_1)	(ϕ_2)	(ϕ_3)	First	Second	First	Second
0.01	0.02	0	1.224584917	0.050801419	−0.144250185	−0.000008502
0	0.01	0.02	1.241218609	0.051491440	−0.143343469	−0.000008497
0.02	0	0.01	1.262961759	0.052393450	−0.135532493	−0.000007991
0.01	0.01	0.01	1.243249735	0.051575701	−0.140954874	−0.000008315
0.02	0.01	0.01	1.266647356	0.052546330	−0.140804066	−0.000008298
0.03	0.01	0.01	1.287934365	0.053429407	−0.140656140	−0.000008288
0.01	0.02	0.01	1.247206247	0.051739853	−0.146365895	−0.000008627
0.01	0.03	0.01	1.249896997	0.051851470	−0.1518636795	−0.000008949
0.01	0.01	0.02	1.266451055	0.052538193	−0.143085694	−0.000008443
0.01	0.01	0.03	1.289887447	0.053510443	−0.145229864	−0.000008573

Figures 7–9 show the influence of various value of ϕ_3 on velocity profile, $f'(\eta)$ and $g'(\eta)$, and temperature profile, $\theta(\eta)$. The value of nanoparticle ϕ_3 used in the graphs are $0, 0.01$ and 0.02 while ϕ_1 and ϕ_2 are both set to 0.01 and $S = 0$. It clearly shows that as the value of ϕ_3 increases, there is a corresponding lower both velocity profile, $f'(\eta)$ and $g'(\eta)$ and a higher temperature profile. Furthermore, it is observed that all the velocity and temperature profiles satisfied the boundary condition (10) asymptotically.
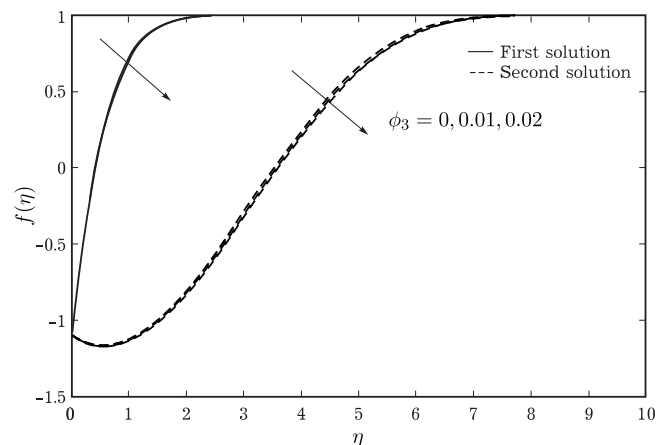
In this research, the oblique stagnation-point flow of a ternary hybrid nanofluid towards a shrinking surface was investigated. A similarity transformation was used to convert the partial differential equations (PDEs) into ordinary differential equations (ODEs), which were then solved numerically. The numerical results were presented graphically for specific parameter values using the bvp4c solver in MATLAB software.
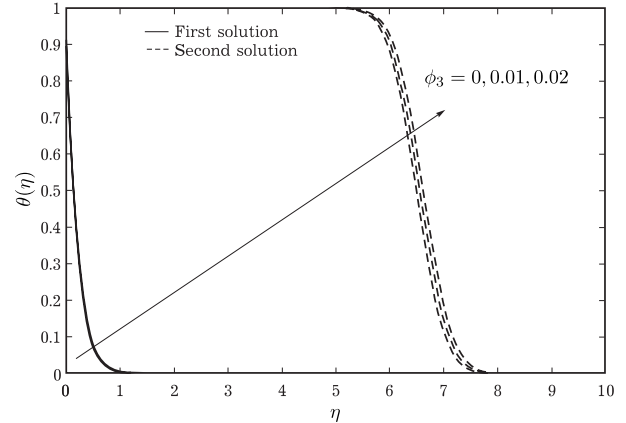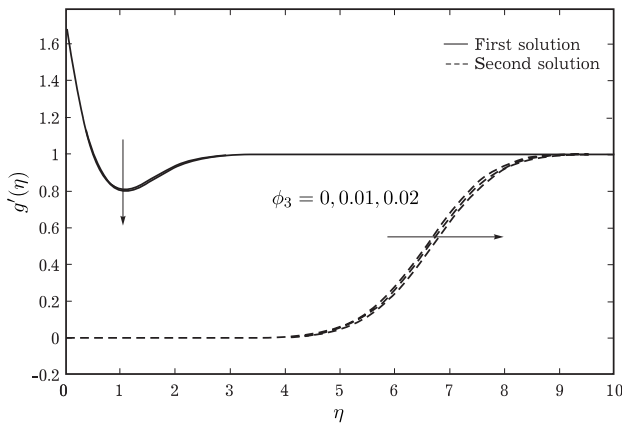

Fig. 7. Effect of various ϕ_3 on velocity profile $f'(\eta)$.

Fig. 8. Effect of various ϕ_3 on velocity profile $g'(\eta)$. **Fig. 9.** Effect of various ϕ_3 on temperature profile $\theta(\eta)$.

The research involving these three different nanoparticles provided valuable insights into their impact on the fluid dynamics and heat transfer characteristics of the system. The findings indicate that as the concentration of these nanoparticles increases, there is a notable impact on both the Nusselt number and skin friction. The enhanced thermal conductivity and surface area of the nanoparticles led to improved heat transfer capabilities, as evidenced by an increase in the Nusselt number. The relationship between nanoparticle concentration, the Nusselt number, and skin friction depends on various factors, including the concentration, size, and properties of the nanoparticles, as well as the specific characteristics of the flow and heat transfer conditions.

The suction parameter positively influences both normal and shear flow velocity profiles. The application of suction in this flow scenario delays boundary layer separation, enhancing the heat transfer rate at the shrinking surface. Although the temperature profile and thermal boundary layer thickness decrease with the introduction of suction, the heat transfer rate increases.

[1] Hiemenz K. Die Grenzschicht an einem in den gleichformigen Flussigkeitsstrom eingetauchten geraden Kreiszylinder. Dingler's Polytechical Journal. **326**, 321–324 (1911).

[2] Mahapatra T. R., Nandy S. K., Gupta A. S. Oblique stagnation-point flow and heat transfer towards a shrinking sheet with thermal radiation. Meccanica. **47** (6), 1325–1335 (2012).

[3] Rahman M. M., Grosan T., Pop I. Oblique stagnation-point flow of a nanofluid past a shrinking sheet. International Journal of Numerical Methods for Heat & Fluid Flow. **26** (1), 189–213 (2016).

[4] Khan M. R. Numerical analysis of oblique stagnation point flow of nanofluid over a curved stretching/shrinking surface. Physica Scripta. **95** (10), 105704 (2020).

[5] Suresh S., Venkitaraj K. P., Selvakumar P., Chandrasekar M. Effect of Al_2O_3-Cu/water hybrid nanofluid in heat transfer. Experimental Thermal and Fluid Science. **38**, 54–60 (2012).

[6] Sidik N. A. C., Adamu I. M., Jamil M. M., Kefayati G. H. R., Mamat R., Najafi G. Recent progress on hybrid nanofluids in heat transfer applications: A comprehensive review. International Communications in Heat and Mass Transfer. **78**, 68–79 (2016).

[7] Abuzar G., Tariq J., Fotini L. Oblique stagnation point flow of a non-Newtonian nanofluid over stretching surface with radiation: A numerical study. Thermal Science. **21** (5), 2139–2153 (2017).

[8] Devi S. U., Devi S. A. Heat transfer enhancement of Cu-Al_2O_3/water hybrid nanofluid flow over a stretching sheet. Journal of the Nigerian Mathematical Society. **36** (2), 419–433 (2017).

[9] Hayat T., Nadeem S., Khan A. U. Rotating flow of Ag-CuO/H_2O hybrid nanofluid with radiation and partial slip boundary effects. The European Physical Journal E. **41** (6), 75 (2018).

[10] Li X., Khan A. U., Khan M. R., Nadeem S., Khan S. U. Oblique Stagnation Point Flow of Nanofluids over Stretching/Shrinking Sheet with Cattaneo–Christov Heat Flux Model: Existence of Dual Solution. Symmetry. **11** (9), 1070 (2019).

[11] Oke A. S., Fatunmbi E. O., Animasaun I. L., Juma B. A. Exploration of ternary-hybrid nanofluid experiencing Coriolis and Lorentz forces: case of three-dimensional flow of water conveying carbon nanotubes, graphene, and alumina nanoparticles. Waves in Random and Complex Media. 1–20 (2022).

[12] Mahmood Z., Khan U. Unsteady three-dimensional nodal stagnation point flow of polymer-based ternary-hybrid nanofluid past a stretching surface with suction and heat source. Science Progress. **106** (1), (2023).

[13] Sajid T., Pasha A. A., Jamshed W., Shahzad F., Eid M. R., Ibrahim R. W., El Din S. M. Radiative and porosity effects of trihybrid Casson nanofluids with Bödewadt flow and inconstant heat source by Yamada–Ota and Xue models. Alexandria Engineering Journal. **66**, 457–473 (2023).

[14] Mahmood Z., Khan U., Saleem S., Rafique K., Eldin S. M. Numerical analysis of ternary hybrid nanofluid flow over a stagnation region of stretching/shrinking curved surface with suction and Lorentz force. Journal of Magnetism and Magnetic Materials. **573**, 170654 (2023).

[15] Yahaya R. I., Arifin N. M., Pop I., Ali F. M., Isa S. S. P. M. Dual solutions for the oblique stagnation-point flow of hybrid nanofluid towards a shrinking surface: Effects of suction. Chinese Journal of Physics. **81**, 193–205 (2023).

[16] Mahmood Z., Iqbal Z., Alyami M. A., Alqahtani B., Yassen M. F., Khan U. Influence of suction and heat source on MHD stagnation point flow of ternary hybrid nanofluid over convectively heated stretching/shrinking cylinder. Advances in Mechanical Engineering. **14** (9), (2022).

Похилий потік потрійного гібридного нанофлюїду в точці застою до поверхні, що стискається

Розаіді Н. Л.[1], Хафідзуддін М. Е. Г.[1,2], Аріфін Н. М.[1], Аб Гані А.[1]

[1]*Кафедра математики та статистики Університету Путра Малайзії,*
43400 Серданг, Селангор, Малайзія
[2]*Центр фундаментальних досліджень у галузі науки Університету Путра Малайзії,*
43400 Серданг, Селангор, Малайзія

У цій статті чисельно досліджено похилий потік у точці застою потрійного гібридного нанофлюїду до поверхні, що стискається. Перетворення подібності було використано для перетворення керівних рівнянь у набір звичайних диференціальних рівнянь, які розв'язано чисельно за допомогою bvp4c у програмному застосунку MATLAB. Дослідження за участю трьох різних наночастинок дало цінну інформацію про їхній вплив на динаміку рідини та характеристики теплообміну досліджуваної системи. Вплив параметрів S, λ та об'ємної частки наночастинок на профілі швидкості та температури, локальне поверхневе тертя та локальне число Нуссельта обговорено та представлено в табличному та графічному вигляді. Виявлено, що вищі концентрації наночастинок призводять до збільшення опору потоку, конвекції та швидкості теплопередачі.

Ключові слова: *природний конвекційний потік, гібридний нанофлюїд* Al_2O_3-*Cu/вода, квадратна порожнина, метод скінченних елементів, форма наночастинок.*